

Thermal Instability in Clusters of Galaxies with Conduction

Woong-Tae Kim and Ramesh Narayan

*Harvard-Smithsonian Center for Astrophysics,
60 Garden Street, Cambridge, MA 02138*

wkim@cfa.harvard.edu, narayan@cfa.harvard.edu

ABSTRACT

We consider a model of galaxy clusters in which the hot gas is in hydrostatic equilibrium and maintains energy balance between radiative cooling and heating by thermal conduction. We analyze the thermal stability of the gas using a Lagrangian perturbation analysis. For thermal conductivity at the level of $\sim 20 - 40\%$ of Spitzer conductivity, consistent with previous estimates for cluster gas, we find that the growth rate of the most unstable global radial mode is $\sim 6-9$ times lower than the growth rate of local isobaric modes at the cluster center in the absence of conduction. The growth time in typical clusters is $\sim 2 - 5$ Gyr, which is comparable to the time since the last major merger episode, when the gas was presumably well mixed. Thus, we suggest that thermal instability is not dynamically significant in clusters, provided there is an adequate level of thermal conduction. On the other hand, if the heating of the gas is not the result of thermal conduction or any other diffusive process such as turbulent mixing, then the thermal instability has a growth time under a Gyr in the central regions of the cluster and is a serious threat to equilibrium. We also analyze local nonradial modes and show that the Lagrangian technique leads to the same dispersion relation as the Eulerian approach, provided that clusters are initially in strict thermal equilibrium. Because cluster gas is convectively stable, nonradial modes always have a smaller growth rate than equivalent radial modes.

Subject headings: galaxies: clusters — cooling flows — X-rays: galaxies — conduction — hydrodynamics — instability

1. Introduction

Galaxy clusters contain a large amount of hot diffuse gas radiating prolifically in thermal X-rays. In the absence of heat sources, the radiative cooling due to this emission should induce a subsonic inflow of gas in the central regions, leading to substantial condensation of cold gas in rich clusters (e.g., Fabian 1994 and references therein). However, recent high-resolution X-ray data from *XMM-Newton* and *Chandra* reveal no evidence for such cooling flows, nor any significant evidence for mass dropout. In particular, there is no evidence for gas at temperatures below about a third of the average temperature (Peterson et al. 2001, 2003; Tamura et al. 2001; Böhringer et al. 2001; Fabian et al. 2001a; Molendi & Pizzolato 2001; Matsushita et al. 2002; Johnstone et al. 2002), suggesting that there must be some heat source (or sources) that prevents the gas from cooling below this limit. Candidate heating mechanisms include radiative and mechanical power from active galactic nuclei (AGN) (Ciotti & Ostriker 2001; Churazov et al. 2002; Brüggén & Kaiser 2002; Reynolds, Heinz, & Begelman 2002; Kaiser & Binney 2003), thermal conduction from the hotter outer regions of the cluster to the center (Narayan & Medvedev 2001; Fabian, Voigt, & Morris 2002; Gruzinov 2002; Zakamska & Narayan 2003, hereafter ZN03), or perhaps both (e.g., ZN03, Ruszkowski & Begelman 2002; Brighenti & Mathews 2002, 2003).

The effects of conduction in clusters have been widely discussed by many authors (e.g., Binney & Cowie 1981; Tucker & Rosner 1983; Bertschinger & Meiksin 1986; Bregman & David 1988; Gaetz 1989; Rosner & Tucker 1989; David et al. 1992; Pistinner & Shaviv 1996; see Fabian 1994 and references therein). It was shown that thermal conduction, when unimpeded, can significantly reduce inferred mass deposition rates in cooling flow clusters (Bertschinger & Meiksin 1986; Rosner & Tucker 1989), although such systems may end up being almost isothermal (Bregman & David 1988). Nevertheless, thermal conduction was considered to be unimportant in galaxy clusters as it was believed that, in the presence of magnetic fields, the cross-field diffusion coefficient would be negligibly small. Since magnetic fields are ubiquitous in clusters (e.g., Carilli & Taylor 2002), it appeared that the effective isotropic conduction coefficient κ in the presence of magnetic fields would be smaller by orders of magnitude than the classical Spitzer (1962) value, κ_{Sp} , of an unmagnetized plasma.

Narayan & Medvedev (2001) recently showed that cross-field diffusion of electrons is quite efficient if magnetic fields are fully turbulent and have a wide range of coherence length scales. Extending earlier work by Rechester & Rosenbluth (1978), Chandran & Cowley (1998), Chandran et al. (1999), and Malyshkin & Kulsrud (2001), and adopting the model of Goldreich & Sridhar (1995, 1997) for MHD turbulence, Narayan & Medvedev (2001) estimated that $f \equiv \kappa/\kappa_{\text{Sp}} \sim 0.2$ in a turbulent magnetized plasma. Very recently, Cho et al. (2003) have used direct numerical simulations to show that the turbulent diffusion of a

scalar field in MHD turbulence is as efficient as, or perhaps even more efficient than, the prediction of Narayan & Medvedev (2001). These studies have led to the revival of the idea that conduction might be an important heating source in clusters.

The viability of thermal conduction as a heating mechanism has found support in the work of Voigt et al. (2002), Fabian, Voigt, & Morris (2002), and ZN03, who showed that the level of conductivity needed to fit the observed temperature distributions of X-ray clusters is consistent with the theoretical estimate of Narayan & Medvedev (2001). In particular, ZN03 explicitly solved the equations for hydrostatic equilibrium and energy balance between radiative cooling and conductive heating and showed that conduction with $f \sim 0.2 - 0.4$ provides reasonable profiles of density and temperature for several clusters. A similar result was also obtained by Brighenti & Mathews (2003) using numerical simulations. Although other heating sources, including AGN jets, cannot be ruled out, these studies suggest that an energy balance based purely on conduction is not unreasonable.

While the above studies show that it is possible to construct equilibrium cluster models with conductive and/or AGN heating, there is no guarantee that the equilibrium will be stable. This is because hot, optically-thin, X-ray-emitting gas is well-known to be thermally unstable (Field 1965). Since the growth time of the thermal instability is comparable to the cooling time (e.g., Fabian 1994), one might expect rapid mass dropout as a result of the instability, even when there is a source of heat to eliminate the classic cooling flow. On the other hand, the absence of any evidence for gas below a few keV in clusters implies that the instability is either absent or very slow. A likely reason for the lack of instability is thermal conduction, which is known to suppress thermal instability on small scales (see, e.g., Field 1965; Defouw 1970; Malagoli et al. 1987; McKee & Begelman 1990; ZN03). However, all previous analyses of this process have been limited to local WKB-type perturbations, where the wavelength of the perturbations is much smaller than the local radius of the system. ZN03 found from their WKB analysis the intriguing result that perturbations with wavelengths up to almost the radius are stable, but that longer wavelengths are probably unstable. Such large-scale variations can be analyzed only through a full global mode analysis, which has not been done so far.

In this paper we present a detailed and formal analysis of local and global modes of thermal instability in equilibrium galaxy clusters with conduction. In §2, we describe the basic equations we solve and present equilibrium solutions for our fiducial model cluster. In §3, we carry out a linear stability analysis of the assumed equilibrium and calculate the global radial modes of the system. We show that there is a single unstable mode, whose growth rate is much lower than the usual thermal instability growth rate in the absence of conduction. In §4, we confirm the main results by means of numerical simulations which show

the development of the thermal instability under various assumptions. In §5, we consider the stability of nonradial modes and clarify a few points on which there has been confusion in the literature. We conclude in §6 with a brief summary of the results and a discussion of the implications.

2. Perturbed Equations

2.1. Basic Equations

We consider the thermodynamic evolution of a hot plasma subject to radiative cooling and thermal conduction. We do not consider any dynamical effects of magnetic fields. We also neglect the self-gravity of the gas which is generally weaker than the gravity of the dark matter.¹ The governing hydrodynamic equations are

$$\frac{d\rho}{dt} + \rho \nabla \cdot \mathbf{v} = 0, \quad (1)$$

$$\frac{d\mathbf{v}}{dt} + \frac{1}{\rho} \nabla P + \nabla \Phi = 0, \quad (2)$$

$$\frac{1}{\gamma - 1} \frac{dP}{dt} - \frac{\gamma}{\gamma - 1} \frac{P}{\rho} \frac{d\rho}{dt} + \rho \mathcal{L} + \nabla \cdot \mathbf{F} = 0. \quad (3)$$

Here, $d/dt \equiv \partial/\partial t + \mathbf{v} \cdot \nabla$ is the Lagrangian time derivative, ρ is the mass density, \mathbf{v} is the velocity, T is the temperature, Φ is the gravitational potential, $\gamma = 5/3$ is the adiabatic index of the gas, $\rho \mathcal{L} = 2.1 \times 10^{-27} n_e^2 T^{1/2}$ erg cm⁻³ s⁻¹ is the energy loss rate per unit volume due to thermal bremsstrahlung (Rybicki & Lightman 1979; ZN03), and P is the thermal pressure for which we adopt the equation of state of an ideal gas,

$$P = \frac{\rho k_B T}{\mu m_u} = \frac{\mu_e}{\mu} n_e k_B T, \quad (4)$$

where m_u is the atomic mass unit, n_e is the electron number density, and μ and μ_e denote the mean molecular weight per hydrogen atom and per electron, respectively. We use $\mu = 0.62$ and $\mu_e = 1.18$, corresponding to a fully ionized gas with hydrogen fraction $X = 0.7$ and helium fraction $Y = 0.28$ (ZN03).

In equation (3), the conductive heat flux \mathbf{F} is determined by

$$\mathbf{F} = -\kappa \nabla T, \quad (5)$$

¹We found that the explicit inclusion of self-gravity increases the growth rates of global thermal instability by only ~ 3 % from the non-self-gravitating values.

where the conductivity κ is a fraction f of the classical Spitzer (1962) conductivity κ_{Sp} ,

$$\kappa = f\kappa_{\text{Sp}} = f \frac{1.84 \times 10^{-5} T^{5/2}}{\ln \Lambda_C} \text{ erg s}^{-1} \text{ K}^{-1} \text{ cm}^{-1}, \quad (6)$$

with the Coulomb logarithm $\ln \Lambda_C \sim 37$. We do not consider nonlocal heat transport as in the model of Chun & Rosner (1993). In an unmagnetized plasma, conduction is isotropic and f is unity. The presence of a magnetic field generally reduces f by resisting motions of thermal electrons across the field lines. Although the suppression of κ would be very high if magnetic fields are uniform or only moderately tangled (e.g., Chandran & Cowley 1998), Narayan & Medvedev (2001) showed that $f \sim 0.2$ in a fully turbulent plasma medium in which magnetic fields are chaotic over a wide range of length scales. In this paper, we assume that f is constant in both space and time.

We use the NFW form of the dark matter distribution ρ_{DM} to determine the gravitational potential Φ through

$$\nabla^2 \Phi = 4\pi G \rho_{\text{DM}}(r) = \frac{2GM_0}{(r+r_c)(r+r_s)^2}, \quad (7)$$

with a softened core radius r_c , a scale radius r_s , and a characteristic mass M_0 . Utilizing the mass-temperature relation of Afshordi & Cen (2002) and the mass-scale relation of Maoz et al. (1997), we determine M_0 and r_s for a given cluster from the observed temperature in the outer regions of the cluster (see ZN03). For r_c , which determines the shape of the potential in the very inner parts, we adopt the best-fit values (either $r_c = 0$ or $r_c = r_s/20$) recommended by ZN03.

Without any heating source to compensate for X-ray cooling, a cluster would lose its thermal energy at a rate $\rho\mathcal{L}$. Assuming that cooling occurs at fixed pressure, we may define from equation (3) the isobaric cooling time²

$$t_{\text{cool}} \equiv \frac{\gamma}{\gamma-1} \left(\frac{P}{\rho\mathcal{L}} \right) = 0.96 \text{ Gyr} \left(\frac{n_e}{0.05 \text{ cm}^{-3}} \right)^{-1} \left(\frac{k_B T}{2 \text{ keV}} \right)^{1/2}. \quad (8)$$

Similarly, we define the conduction time as

$$t_{\text{cond}} \equiv \frac{\gamma}{\gamma-1} \left(\frac{\lambda^2 P}{4\pi^2 \kappa T} \right), \quad (9)$$

²Note that the cooling time as defined here is μ_e/μ times longer than the conventional definition, $5k_B T/2n_e\Lambda$, with $\Lambda = \rho\mathcal{L}/n_e^2$ (cf. Sarazin 1988; David et al. 2001). At constant pressure, equation (3) gives $T(t)/T(0) = n_e(0)/n_e(t) = (1 - 3t/2t_{\text{cool}})^{2/3}$.

where λ is the length scale over which the temperature changes appreciably. By comparing equations (8) and (9), we see that conductive heating becomes comparable to radiative cooling at $\lambda \sim \lambda_F$ where

$$\lambda_F \equiv 2\pi \left(\frac{\kappa T}{\rho \mathcal{L}} \right)^{1/2} = 31.4 \text{ kpc} \left(\frac{f}{0.2} \right)^{1/2} \left(\frac{n_e}{0.05 \text{ cm}^{-3}} \right)^{-1} \left(\frac{k_B T}{2 \text{ keV}} \right)^{3/2} \quad (10)$$

is the Field length (Field 1965; McKee & Begelman 1990). This corresponds to the length scale below which thermal conduction erases temperature perturbations completely (Field 1965). Since the length scale for temperature variations is typically $\sim 10 - 100$ kpc, we conclude that thermal conduction with $f \gtrsim 0.1$ can potentially support galaxy clusters against radiative cooling (see Narayan & Medvedev 2001; Fabian, Voigt, & Morris 2002; Gruzinov 2002; ZN03).

2.2. Initial Equilibrium

It is straightforward to find initial equilibrium solutions of equations (1)-(7). We assume that the equilibrium is spherically symmetric, static, and time-independent. Working in spherical coordinates (r, θ, ϕ) , we simplify equations (2), (3), and (5) to

$$\frac{dP}{dr} = -\rho \frac{d\Phi}{dr}, \quad (11)$$

$$\frac{1}{r^2} \frac{d}{dr} (r^2 F_r) = -\rho \mathcal{L}, \quad (12)$$

$$\kappa \frac{dT}{dr} = -F_r, \quad (13)$$

where F_r denotes the radial heat flux.

Full numerical solutions of the differential equations (7) and (11)-(13) were presented by ZN03. They varied f to find the solutions that give the best fits to the observed density and temperature profiles of ten clusters. They found that thermal conduction with $f \sim 0.2 - 0.4$ explains the density and temperature distributions of five clusters fairly well (A1795, A1835, A2199, A2390, RXJ1347.5-1145). However, five other clusters require unphysically large values of f , indicating that those clusters are incompatible with a pure conduction model and require other heat sources. In this paper we take the best-fit parameters obtained by ZN03 for the five clusters that are consistent with conduction, and we analyze their stability to global radial modes. Table 1 lists the model parameters and various time scales. We adopt the cluster A1795 as our fiducial model.

Figure 1 illustrates an equilibrium solution for A1795. The temperature is minimum at $r = 0$ and begins to rise sharply at $r \sim 5$ kpc. Expansion of the variables near the center gives $T(r) \sim T_0 + (\rho_0 \mathcal{L}_0 / 6\kappa_0) r^2$, where the subscript “0” indicates the values at the center. Therefore, stronger cooling or smaller conductivity would cause the temperature to increase faster. Notice that the temperature is always an increasing function of the radius. Radial heat influx is largest at $r \sim 50$ kpc beyond which the low density makes cooling as well as conductive heating unimportant. Figure 1d plots the local isobaric cooling time t_{cool} defined in equation (8) (solid line) and the growth time, t_∞ (see eq. [27]), of local isobaric thermal perturbations without conduction (dashed line), which are compared with the growth time of the global radial mode in the presence of conduction (t_{grow} ; dotted line): we discuss these instability time scales in the next section.

The radial equilibrium profiles of A1795 presented in Figure 1 are close to but not exactly the same as those derived by Etori et al. (2002). Since A1795 is known to contain a cool filament near the center (Fabian et al. 2001b), the real density and temperature distributions are somewhat non-axisymmetric. Our axisymmetric equilibrium model of A1795 should, therefore, be regarded as an idealized version of what is a much more complex distribution of the intracluster medium in A1795. As we will show below, however, the lowest-order radial mode of thermal instability is the fastest growing mode, so that neglecting the non-axisymmetric parts in the background profiles probably does not affect the results significantly.

3. Linear Analyses of Radial Modes

3.1. Lagrangian Perturbations

We linearize equations (1)-(5) in the Lagrangian framework. A Lagrangian perturbation, represented by an operator Δ , is related to an Eulerian perturbation δ in the usual way,

$$\Delta = \delta + \vec{\xi} \cdot \nabla, \quad (14)$$

where the vector $\vec{\xi}$ measures the Lagrangian displacement of a fluid element from its unperturbed location (e.g., Shapiro & Teukolsky 1983). One of the advantages of adopting the Lagrangian approach is that it simplifies the perturbed equations greatly. For instance, the perturbed continuity equation (1) becomes

$$\Delta\rho = -\rho\nabla \cdot \vec{\xi}. \quad (15)$$

Nevertheless, both Lagrangian and Eulerian descriptions should give the same results, especially if the initial state is static and in complete equilibrium. Various properties of Δ and

the commutation relations associated with Δ and δ can be found in Shapiro & Teukolsky (1983).

We assume that the perturbations are all radial. Applying Δ to equations (2)-(5) and using equation (15), we obtain

$$\frac{d^2 \xi_r}{dt^2} = \frac{P}{\rho} \frac{\partial}{\partial r} \left(\frac{1}{r^2} \frac{\partial r^2 \xi_r}{\partial r} \right) - \frac{1}{\rho} \frac{\partial}{\partial r} \left(P \frac{\Delta T}{T} \right) - \frac{\partial}{\partial r} \left(\xi_r \frac{d\Phi}{dr} \right), \quad (16)$$

$$\frac{1}{4\pi r^2} \frac{\partial}{\partial r} \Delta L_r = \left(\frac{P}{\gamma - 1} \frac{d}{dt} + \rho T \mathcal{L}_T \right) \frac{\Delta T}{T} + \left(P \frac{d}{dt} - \rho^2 \mathcal{L}_\rho \right) (\nabla \cdot \vec{\xi}), \quad (17)$$

$$\kappa T \frac{\partial}{\partial r} \left(\frac{\Delta T}{T} \right) = F_r \left(\frac{\Delta \kappa}{\kappa} + \frac{\Delta T}{T} - \frac{d\xi_r}{dr} + 2 \frac{\xi_r}{r} \right) + \frac{\Delta L_r}{4\pi r^2}, \quad (18)$$

where $\mathcal{L}_T \equiv \partial \mathcal{L} / \partial T|_\rho$, $\mathcal{L}_\rho \equiv \partial \mathcal{L} / \partial \rho|_T$, ξ_r is the radial component of $\vec{\xi}$, and $L_r \equiv -4\pi r^2 F_r$ is the radial heat luminosity. We use ξ_r , ΔT , and ΔL_r as independent variables.

We seek linear eigenmodes that behave as $\sim e^{\sigma t}$ with time. We then rewrite equations (16)-(18) as

$$\frac{d^2}{dr^2} \left(\frac{\xi_r}{r} \right) + \left(\frac{4}{r} + \frac{d \ln P}{dr} \right) \frac{d}{dr} \left(\frac{\xi_r}{r} \right) + \frac{\rho}{P} \left(\frac{1}{r} \frac{d\Phi}{dr} - 4\pi G \rho_{\text{DM}} - \sigma^2 \right) \frac{\xi_r}{r} = \frac{1}{rP} \frac{d}{dr} \left(P \frac{\Delta T}{T} \right), \quad (19)$$

$$\frac{1}{4\pi r^2} \frac{d}{dr} \Delta L_r = \left(\frac{P\sigma}{\gamma - 1} + \rho T \mathcal{L}_T \right) \frac{\Delta T}{T} + (P\sigma - \rho^2 \mathcal{L}_\rho) \left[r \frac{d}{dr} \left(\frac{\xi_r}{r} \right) + 3 \frac{\xi_r}{r} \right], \quad (20)$$

$$\kappa T \frac{d}{dr} \left(\frac{\Delta T}{T} \right) = F_r \left[\frac{7}{2} \frac{\Delta T}{T} - r \frac{d}{dr} \left(\frac{\xi_r}{r} \right) + \frac{\xi_r}{r} \right] + \frac{\Delta L_r}{4\pi r^2}, \quad (21)$$

which are our desired perturbation equations. This set of ordinary differential equations forms an eigenvalue problem for global modes, with σ as the eigenvalue, which can be solved numerically subject to appropriate boundary conditions. Before considering the full problem, we study local modes that do not depend on boundaries to gain some physical insight.

3.2. Local Radial Modes

Let us consider local WKB perturbations of the form $\sim e^{ik_r r + \sigma t}$ and let us assume that the radial wavenumber k_r satisfies $k_r r \gg 1$, $k_r (d \ln P / dr) \gg 1$. We may then neglect the spherical geometry and ignore local gradients of the background quantities relative to spatial gradients of the perturbed variables. We also assume that $\sigma^2 < P k_r^2 / \rho$, corresponding to

slowly evolving perturbations; this eliminates sound waves from consideration. In this local approximation, equation (19) simplifies to

$$ik_r \xi_r = \frac{\Delta T}{T}, \quad (22)$$

while equations (20) and (21) may be combined to give

$$-(P\sigma - \rho^2 \mathcal{L}_\rho - \rho \mathcal{L}) ik_r \xi_r = \left(\frac{P\sigma}{\gamma - 1} + \rho T \mathcal{L}_T + k_r^2 \kappa T \right) \frac{\Delta T}{T}. \quad (23)$$

Eliminating ξ_r and $\Delta T/T$ from equations (22) and (23), we find

$$\sigma = \sigma_\infty - \frac{\gamma - 1}{\gamma} \frac{\kappa T}{P} k_r^2, \quad (24)$$

where σ_∞ , defined by

$$\sigma_\infty \equiv \frac{\gamma - 1}{\gamma P} (\rho^2 \mathcal{L}_\rho + \rho \mathcal{L} - \rho T \mathcal{L}_T) = -\frac{\gamma - 1}{\gamma} \frac{\rho T}{P} \left(\frac{\partial \mathcal{L}/T}{\partial T} \right)_P, \quad (25)$$

is the growth rate of isobaric thermal perturbations without conduction (Field 1965).

Equation (24) is a local dispersion relation for thermal fluctuations.³ In the absence of conduction, $\sigma = \sigma_\infty$, so that instability develops if the cooling function satisfies the generalized Field criterion

$$\left(\frac{\partial \mathcal{L}/T}{\partial T} \right)_P < 0, \quad (26)$$

for isobaric thermal instability (Balbus 1986). For X-ray emitting clusters of galaxies with $\mathcal{L} \propto \rho T^{1/2}$, the condition (26) is easily met. The corresponding growth time amounts to

$$t_\infty \equiv \sigma_\infty^{-1} = \frac{2}{3} t_{\text{cool}}, \quad (27)$$

suggesting that local radial disturbances will grow slightly faster than the isobaric cooling time of the system. Figure 1*d* plots t_∞ for A1795 as a dashed line.

It is well known that thermal conduction stabilizes short-wavelength perturbations against thermal instability (e.g., Field 1965; Malagoli et al. 1987; McKee & Begelman 1990). It not only reduces growth rates but also suppresses thermal instability completely

³Equation (24) can be obtained by taking the limit of $k_r \gg \rho \sigma^2 / P$ in the dispersion relation (15) of Field (1965) for a uniform medium. Note, however, that the condition $\mathcal{L} = 0$ in his initial equilibrium state gives $\sigma_\infty = -[(\gamma - 1)\rho/\gamma P](\partial \mathcal{L}/\partial T)_P$ instead of equation (25).

if $k_r > (3/2)^{1/2}k_F$, where $k_F = 2\pi/\lambda_F$. The existence of unstable modes, therefore, requires large wavelength perturbations. ZN03 showed that the clusters they studied are thermally stable for all wavelengths up to approximately the radius. The fate of modes with longer wavelengths was unclear in their study since a local analysis is no longer valid. A global analysis is required to study such large scale perturbations. This is the topic of the next subsection.

3.3. Global Solutions

To analyze the global stability problem, we solve equations (19)-(21) numerically. Since these equations are equivalent to four first-order differential equations, we need to specify four boundary conditions. The two inner boundary conditions are

$$\frac{d\xi_r/r}{dr} = 0 \quad \text{and} \quad \frac{\Delta L_r}{4\pi r^2} = 0, \quad \text{at } r = 0. \quad (28)$$

The first condition guarantees that the solutions are regular, while the second condition corresponds to a zero gradient in the perturbed temperature at the center. Since $\xi_r = 0$ at $r = 0$ for radial modes, we fix $\xi_r/r = 1$ as a normalization condition.

The two other boundary conditions come from the outer boundary which we arbitrarily locate at $r_b = 1$ Mpc. Since all eigenfunctions that we have obtained are found to decay rapidly with increasing radius, the solutions are quite insensitive to the particular choice of the outer boundary conditions as well as the location of the outer boundary. This is because the cooling time well exceeds the Hubble time in the outer parts of clusters (Fig. 1d), and so the thermal instability develops very slowly near the outer boundary. The results presented in this paper correspond to the specific boundary conditions

$$\xi_r = 0 \quad \text{and} \quad \Delta T = 0, \quad \text{at } r = r_b. \quad (29)$$

We have tried various other outer boundary conditions such as a fixed pressure, a fixed entropy, etc. The results are unchanged.

The numerical calculations proceed as follows. We first fix σ and integrate equations (19)-(21) from $r = 0$ to $r = r_b$, setting $\alpha \equiv \Delta T/T|_{r=0}$ to an arbitrary value. At the outer boundary, we check the first condition in equation (29), update α using the Newton-Raphson method, and continue iterating until convergence is attained. Then, we scan σ in the range $10^{-6} < |\sigma|r_b/c_0 < 10^2$, where c_0 is the adiabatic sound speed at the cluster center, and use the second condition in equation (29) as a discriminant for solutions. By this procedure, we do not miss any eigensolution. We allow for both real and complex σ .

When σ is real and positive, we find that a cluster with $f \gtrsim 0.2$ has only one unstable global mode. In Figure 2, we plot the eigenfunctions of the unstable mode for all five clusters listed in Table 1. The perturbations have largest amplitude near the center ($r < 1$ kpc) and decay rapidly with increasing radius. This is consistent with the notion that the central regions have a much shorter cooling time and are thus more prone to thermal instability. Note that ξ_r/r has the same sign as $\Delta T/T$, indicating that the thermal instability leads to a mass inflow. We will show in §4 that the mass inflow rate driven by the instability is, however, much lower than that in conventional cooling flows. As the last two columns of Table 1 shows, the growth time of the most unstable global radial modes is typically $\sim 2 - 5$ Gyr, which is about 6 to 9 times longer than that of local isobaric modes at the cluster center in the absence of conduction. This time scale is not much shorter than the age of the system since the last major merger. Therefore, thermal instability in the presence of conduction is unlikely to be a serious threat to clusters.

Why is the growth time t_{grow} of the mode so much longer than the growth time $t_{\infty,0}$ of the local isobaric mode at the cluster center? The reason is that the eigenfunction extends over a considerable range of r , of order tens of kpc (Fig. 2). Over this range, t_{∞} increases from $t_{\infty,0}$ at the center to much larger values (Fig. 1d). Since the growth time of the mode corresponds to an appropriate eigenfunction-weighted volume-average of t_{∞} , and since the averaging is dominated by $r \sim$ tens of kpc, this causes t_{grow} to be significantly larger than $t_{\infty,0}$.

How effectively does conduction stabilize thermal instability? To address this question, we have solved equations (19)-(21) using different values of f for the perturbations. We adopt the same density and temperature distributions as shown in Figure 1, which means that we take the same $f = 0.2$ for the initial unperturbed state. However, we allow f to vary in the perturbations. In Figure 3, we show the resulting mode growth rates σ relative to $\sigma_{\infty,0}$, the central value of the growth rate of local thermal instability without conduction (see eq. [25]). When $f > 5$ (although unphysical), we find that conduction quenches thermal instability completely; that is, there is no unstable mode. For $0.14 < f < 5$, there exists a single unstable mode that has no node in the eigenfunction for ξ_r/r . The case shown in Figure 2, $f = 0.2$, corresponds to this range. When f is below 0.14, a new mode appears and now the system has two unstable modes. Because the new mode has a node in ξ_r/r somewhere inside the cluster, its growth rate is smaller than the zero-node mode, as equation (24) suggests. As f keeps decreasing, new modes having lower growth rates successively emerge. In the limit of zero conduction, there is an infinite number of unstable modes, with the maximum growth rate equal to $\sigma_{\infty,0}$.

Figure 3 shows that over much of the range of f , the growth rate increases very slowly as

f decreases. As before, the reason may be traced to the fact that the eigenfunction extends over a range of r and σ represents a suitable average of σ_∞ over this volume. Thus, even for $f = 0.01$, the fundamental $n = 0$ mode has a growth rate about 4 times smaller than $\sigma_{\infty,0}$. Eigenfunctions become more centrally concentrated as f decreases, and thus a mode with smaller f generally has a larger growth rate, though the increase of σ with decreasing f is rather slow (Fig. 3).

In addition to unstable modes for which thermal conduction plays a stabilizing role, clusters also contain decaying modes with real and negative σ . Figure 4 displays examples of eigenfunctions for a few selected decaying modes and shows the dependence of σ on the reduction factor f . In contrast to unstable modes, which have smaller frequencies as the number of nodes increases, higher-order decaying modes have larger (negative) frequencies. This is consistent with equation (24)⁴, which implies that the presence of decaying modes is a simple manifestation of diffusion ironing out temperature perturbations.

We have searched for global solutions with complex σ , i.e., overstable modes, but found no overstable radial mode with $\text{Re}(\sigma) > 0$ under the imposed boundary conditions. Physically, thermal overstability occurs when sound waves are amplified by absorbing (losing) heat during the compression (rarefaction) phase of oscillations (Field 1965). Since the cooling function for X-ray emitting clusters does not satisfy the isentropic instability criterion of Field (1965), the absence of radial overstability is in fact guaranteed. This leaves pure unstable modes as the sole growing modes. Although some underdamping modes (complex σ with negative real parts) were found, they are of no interest and we do not discuss them further.

4. Nonlinear Evolution of Radial Modes

As a check of the global linear stability analyses described in the previous section, we have solved the full dynamical equations (1)-(7) using a time-dependent approach. Starting with the equilibrium density and temperature profiles of A1795 calculated in §2.2, we have run three models: (model A) a cluster without any heating; (model B) a cluster with no conduction, but constantly heated (by some fictitious agency) at a rate such as to maintain thermal balance in the initial equilibrium; (model C) a cluster with self-consistent conductive heating with $f = 0.2$. Model A simulates the standard cluster cooling flow problem, whereas models B and C are intended to explore the growth of thermal instability from an initial

⁴Since $\sigma \propto -\kappa T k_r^2$ for decaying modes, equation (24), which assumes $\sigma^2 \ll P k_r^2 / \rho$, does not describe higher-order modes very accurately.

equilibrium state, with and without thermal conduction. Note that our adopted cooling function for X-ray free-free emission becomes invalid when the gas in models A-C cools below ~ 1 keV. Nevertheless, these simulations allow us to confirm the growth rates of thermal instability that we computed in §3 and to estimate mass inflow rates resulting from either radiative cooling or thermal instability.

We follow the nonlinear evolution of our model clusters using the ZEUS hydrodynamic code (Stone & Norman 1992). We construct a logarithmically-spaced radial grid, with 500 zones, from $r = 1$ kpc to 1 Mpc, and carry out a one-dimensional simulation. We implement a fully implicit algorithm for thermal conduction in the energy equation (Press et al. 1992). All the variables at both the inner and outer boundaries are assigned to have a vanishing gradient across the boundaries, except for the radial velocity. We fix the radial velocity to be zero at the outer boundary, while allowing it to vary as a linear function of radius at the inner boundary. On the initial equilibrium, we add as a perturbation the most unstable global eigenfunction for density that we found in §3.3, with an amplitude equal to 0.1% of the background density at the cluster center.

Figure 5 shows the evolutionary histories of the maximum density and the mass inflow rate $\dot{M} \equiv -4\pi r^2 \rho v_r$ at $r = 10$ kpc for models A-C. The two dotted lines in Figure 5a represent the analytic estimates for the growth rates of thermal instability with and without conduction; the predictions are in excellent agreement with the results of the numerical simulations. We have also compared the perturbed density and velocity profiles in the linear regime of model C with the corresponding eigenfunctions obtained from the linear theory. Even though the radial grid does not cover the inner 1 kpc, they agree to within $\sim 3\%$. Radial profiles of electron number density, radial velocity, and temperature for a few selected epochs are plotted in Figure 6.

Model A, which is not in equilibrium and is subject to strong radiative cooling, immediately experiences radial inflow of mass everywhere. Although the temperature of the cluster decreases steadily as the gas cools, the thermal pressure does not drop owing to adiabatic compression, which in turn maintains the radial velocity at the level of about $\sim 1 - 2\%$ of the central sound speed until $t \sim 0.6$ Gyr. During this period, we find $n_e \propto T^{-1.05}$ so that the cooling flow is nearly isobaric. As the insert in Figure 5a shows, the maximum density follows the prediction of isobaric cooling fairly well. When the cooling modifies the density and temperature distributions significantly ($t > 0.6$ Gyr), the increased cooling rate in the central parts induces larger mass inflows, causing the central density to increase in a runaway fashion. The change of density and temperature is so rapid that there is no chance for thermal instability to grow. We stop the simulation of model A at $t = 0.85$ Gyr when the central temperature becomes vanishingly small. The mass inflow rate depends rather

sensitively on time and is a linear function of radius for $r < 250$ kpc, with a slope of $\sim 30 M_{\odot} \text{ yr}^{-1} \text{ kpc}^{-1}$, at the end of the run (see Figure 5b).

Models B and C are initially in equilibrium with heating balancing cooling, but they both experience thermal instability. Without conduction, perturbations in model B grow at a rate of $\sigma_{\infty,0} = (0.64 \text{ Gyr})^{-1}$ and become fully unstable within ~ 4 Gyr. Although the growth time of thermal instability in model B is slightly shorter than the isobaric cooling time in model A (see eq. [27]), model B takes a longer time for eventual runaway than model A. This is simply because the former requires the growth of perturbations from a small amplitude, while the latter changes its background state immediately.

Model C clearly illustrates the stabilizing effect of thermal conduction. With $f = 0.2$, conduction causes the maximum growth rate of thermal instability to be about six times smaller than in the nonconducting model B, thereby delaying runaway growth until $t \sim 24$ Gyr (for the particular amplitude of initial perturbations). The mass inflow rate is correspondingly very small throughout its entire evolution. Had we started the evolution with a higher initial perturbation amplitude, it would of course take less time to reach a fully nonlinear state. Small-scale perturbations in real clusters may well have high amplitudes, but they are readily erased by conduction. Since it seems unlikely that the amplitudes of perturbations that are spherically symmetric and coherent over 100 kpc are more than $\sim 10\%$ of background quantities, we believe that galaxy clusters with $f \gtrsim 0.2$ are not likely to exhibit a strong thermal instability for many Gyr.

5. Local Nonradial Modes

We now carry out a local analysis of nonradial Lagrangian perturbations in a static, stratified medium. We do not attempt to solve the full eigenvalue problem for nonradial modes, but instead focus on the local behavior of nonradial modes in the presence of density and/or temperature stratification. Similar work has been reported by White & Sarazin (1987) and Malagoli et al. (1987) who used Eulerian perturbations and showed that a restoring buoyancy force from a stable entropy gradient can change thermal instability into an overstability, confirming the previous results of Defouw (1970). Using Lagrangian perturbations, on the other hand, Balbus (1988) showed that the negative radial gradient of a net cooling function leads to convectively unstable flows in a non-equilibrium system. He further claimed that the Eulerian and Lagrangian approaches give different results, although in a subsequent paper Balbus & Soker (1989) showed that the Lagrangian approach of thermal instability in dynamical media produces results that are apparently consistent with those from the Eulerian analysis (Balbus 2003, private communication). We show below that the

Lagrangian approach in fact gives exactly the same dispersion relation for nonradial thermal instability as the Eulerian analyses referred to above, provided the background is in initial thermal equilibrium.

We use the Lagrangian technique and linearize equations (1)-(5) assuming that perturbations have small amplitudes of the form $\sim Y_{lm}(\theta, \phi)e^{ik_r r + \sigma t}$, where $Y_{lm}(\theta, \phi)$ is the usual spherical harmonic. The detailed procedure to derive a local dispersion relation is given in the Appendix: we write only the final result here,

$$\sigma^3 - \left(\sigma_\infty - \frac{\gamma - 1}{\gamma} \frac{\kappa T}{P} k^2 \right) \sigma^2 + \frac{k_t^2}{k^2} \omega_{\text{BV}}^2 \sigma + \frac{\gamma - 1}{\gamma P} \frac{k_t^2}{k^2} \frac{d\Phi}{dr} \frac{d}{dr} (\rho \mathcal{L} + \nabla \cdot \mathbf{F}) = 0, \quad (30)$$

where $k_t \equiv [l(l+1)]^{1/2}/r$ is the tangential wavenumber, $k^2 = k_r^2 + k_t^2$, and

$$\omega_{\text{BV}}^2 \equiv \frac{d\Phi}{dr} \left(\frac{1}{\gamma} \frac{d \ln P}{dr} - \frac{d \ln \rho}{dr} \right) \quad (31)$$

is the Brunt-Väsälä frequency for convective motions in a radially stratified atmosphere. When the conductivity $\kappa = 0$, equation (30) reduces to equation (3.17) of Balbus (1988)⁵. If $d(\rho \mathcal{L} + \nabla \cdot \mathbf{F})/dr = 0$ in the last term, equation (30) becomes exactly the same as the dispersion relation of the Eulerian approach (Malagoli et al. 1987).

It is the last term in equation (30) that has led to the discrepancy between the Eulerian and Lagrangian perturbation analyses. This term vanishes if the background is in thermal balance, either in the presence of thermal conduction in which case $\rho \mathcal{L} + \nabla \cdot \mathbf{F} = 0$, or with some other sources of heating in which case $\mathcal{L} = 0$ everywhere. If one perturbs equation (3) using the Eulerian operator δ and Lagrangian operator Δ , respectively, and takes the difference of the resulting equations, the residual term is $\vec{\xi} \cdot \nabla (\rho \mathcal{L} + \nabla \cdot \mathbf{F})$. This explains the origin of the last term in equation (30) and the apparent discrepancy of the Eulerian and Lagrangian approaches. The two approaches are consistent with each other only if the background state is in strict thermal equilibrium.

One may argue that the assumption of initial thermal equilibrium is very special and a local analysis can be carried out even in a non-equilibrium system. However, such an analysis would be misleading unless the change of the background state either is allowed for in doing the perturbations or occurs slowly compared to the growth of perturbations

⁵Since Balbus (1988) took $\rho \mathcal{L} \neq 0$ in an initial state, it is unclear how to compute an effective adiabatic index Γ_1 in his notation. Applying Δ directly to his equation (2.1c), one obtains $\Gamma_1 = (5\sigma/2 + \tau \Theta_{\tau, P}) / (3\sigma/2 + \Theta + \Theta_{\tau, P})$ instead of his equation (2.8). Plugging this expression into his equation (3.17) would produce exactly the same local dispersion relation as our equation (30) when $\kappa = 0$. Then, the condition $d\Theta/dr < 0$ in his equation (3.28) is replaced by $d(\rho \mathcal{L})/dr < 0$.

of interest. As we showed in §3, the cooling time in galaxy clusters is comparable to the growth time of thermal instability. Moreover, in §4, we performed a numerical simulation of a cluster that is initially out of thermal equilibrium (model A) and showed that the resulting cooling flow quickly dominates the cluster evolution, leaving no time for the development of a local thermal instability.

Since we assume the system is in initial thermal balance, we rewrite equation (30) as

$$\sigma^2 - \left(\sigma_\infty - \frac{\gamma - 1}{\gamma} \frac{\kappa T}{P} k^2 \right) \sigma + \frac{k_t^2}{k^2} \omega_{\text{BV}}^2 = 0, \quad (32)$$

which was already derived and discussed by Malagoli et al. (1987). Compared to equation (24) for radial perturbations, equation (32) has an extra term that arises from the local buoyancy force. Since $dT/dr > 0$ and $dP/dr < 0$, therefore $\omega_{\text{BV}}^2 > 0$, and galaxy clusters are stable to convective instability. The buoyancy term has then a stabilizing effect, reducing the growth rate of the thermal instability and even altering the character of the instability to an overstability when k_t/k is high enough (Defouw 1970; Malagoli et al. 1987). If a medium is thermally overstable, a bubble that is displaced radially outward (inward) becomes more (less) dense compared to the adiabatic case, thus experiencing an increase of its oscillation amplitude with time.

From equations (24) and (32), it is trivial to show that for a given wave-vector \mathbf{k} , $\text{Re}(\sigma)$ of the local nonradial mode is always smaller than that of the local radial mode (e.g., White & Sarazin 1987), implying that the latter is more unstable. This suggests that global nonradial modes, if they exist, would have smaller growth rates compared to global radial modes.

6. Summary and Discussion

Narayan & Medvedev (2001) and Cho et al. (2003) have shown that thermal conduction is quite efficient in a fully turbulent, magnetized plasma. The diffusion coefficient in such a medium is approximately a fraction $f \sim$ a few tenths of the Spitzer coefficient (the full Spitzer coefficient applies to an unmagnetized medium). Conduction at this level is sufficient to provide significant heat to the cooling gas in a galaxy cluster and to maintain energy balance in the cluster center (Narayan & Medvedev 2001; Voigt et al. 2002; Fabian, Voigt, & Morris 2002; ZN03). This is an attractive explanation for the suppression of mass dropout in cooling cores of clusters. However, the demonstration that one can build equilibrium models with heating equal to cooling is not sufficient, since the hot gas is likely to be subject to a thermal instability (Field 1965). To be fully consistent with the new X-ray data on clusters, which show the absence of gas below a few keV, it is necessary to demonstrate that the thermal instability is either fully suppressed or is at least much weaker than expected.

It is well-known that thermal conduction suppresses thermal instability in a hot gas for perturbations with short wavelengths. Indeed, using a local WKB-like analysis, ZN03 have shown that perturbations with wavelengths up to a fraction of the radius are thermally stable in clusters. However, this still leaves open the possibility that one or more long-wavelength global modes may be unstable. In this paper, we have analyzed in some detail the stability of such global modes.

Following ZN03, we set up the equilibrium density and temperature profiles of clusters, assuming strict hydrostatic and energy equilibrium (§2). By applying Lagrangian perturbations, we derive a set of differential equations that describe the eigenvalue problem for global radial modes, with the mode growth rate σ acting as the eigenvalue (eqs. [19]–[21], §3). In the absence of conduction ($f = 0$), we find as expected that a cluster has an infinite number of unstable modes, all with rapid growth rates $\sigma \sim \sigma_\infty = 1/t_\infty$ (eqs. [24] and [27]), where t_∞ is the standard growth time scale associated with the thermal instability. For typical cooling flow clusters, the modes should grow in less than a Gyr, implying a serious threat to stability. However, when we set $f = 0.2$, roughly the value recommended by Narayan & Medvedev (2001) and ZN03, we find that all radial modes except one become stable. The one residual unstable mode is the fundamental nodeless (in ξ_r/r) mode, i.e. the mode with the longest possible “wavelength” that can fit within the system. This mode is weakly unstable, with a growth time scale t_{grow} that is 6 to 9 times longer than t_∞ . Soker (2003) has recently posted a paper in which he describes a quasi-global stability analysis of clusters. However, both the initial equilibrium he assumes and the perturbations he considers are very approximate, and it is hard to compare his results with ours.

For the clusters we have studied, t_{grow} for the lone unstable mode is $\sim 2 - 5$ Gyr (Table 1). This is an interestingly long time scale, which is probably comparable to the elapsed time since the last major merger event in a hierarchical clustering scenario (typically ~ 7 Gyr for massive clusters, e.g., Kitayama & Suto 1996). We imagine that major mergers (and perhaps to a lesser extent even minor mergers) leave the cluster gas in a highly mixed and turbulent state. If the merger drives the whole system well out of thermal equilibrium, mass dropout would occur very rapidly (< 1 Gyr) at the central parts (as in model A in §4), which may in turn allow the remaining gas to achieve a new thermal equilibrium that is similar to its present state. In a sense, the merger acts to reset initial conditions. After the merger, the unstable global radial mode would grow. However, if the growth time for the mode is comparable to the effective age of the cluster since the last merger, as appears to be the case for our models, then we do not expect the thermal instability to be a major problem.

We have confirmed the results of §3 by means of numerical simulations of radial perturbations in a model cluster (§4, Fig. 5). Three models are discussed. Model A considers a

cluster without any heating to balance cooling. This model exhibits the classic cooling flow catastrophe, a violent and very rapid runaway at the cluster center. The runaway is so rapid that there is no possibility for the thermal instability to do anything. Model C considers a cluster in which cooling is exactly balanced by conductive heating in equilibrium. The numerical simulation shows that this model has a slow instability that grows at precisely the rate calculated in §3. For the particular initial conditions selected, the mode grows to the non-linear runaway stage only after 24 Gyr, which means that the model is for all practical purposes stable. Model B is an interesting in-between case in which heating and cooling are balanced, except that the heating is not from conduction but from some other local (unspecified) agency. This model shows the classic thermal instability. The perturbations grow quite rapidly, on the time scale t_∞ of the Field (1965) instability. In 4 Gyr, the model is completely destroyed by nonlinear runaway.

We thus reach the following important conclusion from the simulations: apart from balancing heating and cooling, it is necessary also to make sure that the heating is of the right kind to control the thermal instability. Specifically, the heating must involve diffusive transport of energy so that short-wavelength perturbations are smoothed out and not allowed to grow, and even long-wavelength perturbations are partially stabilized. Thermal conduction is diffusive in nature and is quite effective in this respect, as we have shown in this paper. Turbulent mixing would be similarly effective. AGN heating via a jet might behave diffusively if the heat is transferred to the cluster gas via mechanical turbulence. Heating through mass infall in minor mergers might also be effective since in this case again the heat is likely to spread through the gas via turbulence. However, radiative heating (Ciotti & Ostriker 2001) or cosmic ray heating (Loewenstein, Zweibel, & Begelman 1991) from an AGN are unlikely to control the thermal instability, since these heating mechanisms are not diffusive in nature.

In this connection, we note that not all solutions to the cooling flow problem involve equilibrium models. Kaiser & Binney (2003) have described an interesting model involving AGN heating in which the gas goes through a limit cycle. For most of the time, the AGN at the center is in quiescence and the gas is not significantly heated. As the gas undergoes a cooling catastrophe, the gas density around the AGN increases, causing the AGN to switch on, to eject a powerful jet and to heat the cluster gas. The heated gas expands, the AGN switches off, and the gas starts the cycle again. The analysis we have carried out in this paper does not include such scenarios, since we have explicitly assumed that heating and cooling are balanced.

In §5, we analyze the properties of nonradial perturbations in a cluster. This problem has been studied by Defouw (1970), White & Sarazin (1987), and Malagoli et al. (1987)

using an Eulerian approach, and by Balbus (1988) using a Lagrangian approach. We show that the Lagrangian analysis leads to the same local dispersion relation (see eq. [32]) as the previous Eulerian analyses, provided that the background is in thermal equilibrium. For a cluster that is convectively stable (as all clusters are), $\omega_{\text{BV}}^2 > 0$ (eq. [31]), and the buoyancy force associated with the entropy gradient plays a stabilizing role. As a result, if we consider radial perturbations with a given wave-vector that are thermally unstable, then non-radial perturbations with the same wave-vector always have a lower growth rate. This means that the most unstable mode is always a radial mode. Although this result is obtained via a local analysis, it is expected to be true for global modes as well. We have, therefore, not analyzed global non-radial modes.

Is it an accident that the mode growth time that we have estimated is comparable to the age of the system as measured since the last major merger? We suggest that perhaps it is not. Imagine a cluster that is formed with sufficient gas such that several modes are initially thermally unstable with fairly short growth times. If the cluster were to start from a well-stirred initial state (say immediately after a merger), the various modes would grow and when the age of the system exceeds the growth time of any particular mode, that mode would go non-linear and cause a certain amount of mass to cool and drop out from the hot medium. The mass dropout will cause the amount of gas in the hot phase to decrease, and as a result, the other modes would become less unstable. With continued mass dropout, perhaps only one unstable mode would be left finally. This mode would remain in the system so long as its growth time is not much shorter than the current age. With increasing age, presumably this mode too will cause some mass dropout, but always in such a manner that the gas that is left will have a growth time comparable to the age. In this picture, mass dropout acts as a safety valve that enables the system to be always in a state of marginal equilibrium. If this scenario is valid, then it is of course natural that the clusters we observe have unstable modes with growth times of order several Gyr.

In this paper, we have assumed the parameter f to be constant over the entire volume of a cluster. This may not be a good approximation in some clusters that exhibit sharp discontinuities in temperature and density (e.g., Markevitch et al. 2000; Vikhlinin et al. 2001a,b; Dupke & White 2003). These cold fronts, located at about $r \sim 300$ kpc, probably result from cluster mergers. Vikhlinin et al. (2001b) argued that strong magnetic fields parallel to cold fronts may be responsible for the low conductivity. If so, the existence of cold fronts is unlikely to affect the strong stabilizing role played by conduction for the bulk of the cluster gas. The cold fronts are presumably transient features, surviving for only a dynamical time (< 1 Gyr) before being disrupted by Kelvin-Helmholtz instability (Mazzotta et al. 2002) or by merger shocks (Nagai & Kravtsov 2003).

From spatial variations of temperature detected in the cluster A754, Markevitch et al. (2003) argued that, in addition to cold fronts, the bulk of the gas in this cluster may have conductivity much smaller than the Spitzer value. The critical question is how recently were the observed temperature inhomogeneities formed and how much longer will they last. If the cluster is undergoing a merger, for instance, the density and temperature fluctuations are all transient. Although conduction tries to smooth out local temperature fluctuations, these structures may be continuously created by subsequent mergers and/or the sloshing motion of the gas in the dark matter potential (Roettiger et al. 1998). Acoustic motions of the gas may also induce temporary fluctuations.

Since a large fraction of galaxy clusters exhibit powerful extended radio sources at their centers, many authors have considered outbursts from the central AGN to be the source of heat to balance the radiative cooling in clusters. As noted above, this works best if the heating is done via some turbulent agency so that short wavelength thermal instability can be controlled. In addition, the AGN heating cannot be too strong since it would smooth out and erase the radial variations of metallicity that have been observed in some clusters (e.g., Allen et al. 2001; Johnstone et al. 2002).

A very real possibility is that both AGN heating and conductive heating work together in clusters, though their relative importance may vary from cluster to cluster (ZN03). It is even possible that AGN heating dominates in the inner regions, while conduction plays a more important role farther out. Recently, Ruszkowski & Begelman (2002) and Brighenti & Mathews (2003) demonstrated that simultaneous heating by AGN and thermal conduction produces quasi-static density and temperature profiles that are similar to those of observed clusters. In particular, Brighenti & Mathews (2003) showed that clusters with AGN heating alone exhibit either too high mass accretion rates or unrealistic temperature distributions, while conductive heating with $f \sim 0.35$ alone or together with AGN heating gives reasonable fits to observations. Although the effects of their computational methods (e.g., removal of cold gas out of the computational domain) and prescriptions for the AGN heating are uncertain, their simulations suggest that the stabilization of the hot gas is most likely achieved by conduction. Therefore, even in clusters where AGN heating is dominant, the role of thermal conduction as a stabilizing agent should not be ignored (ZN03).

We gratefully acknowledge helpful discussions with S. Balbus, L. David, G. Field, E. Ostriker, and N. Yoshida. We also thank an anonymous referee for useful comments. This work was supported in part by NASA grant NAG5-10780.

A. Nonradial Modes

In this appendix, we linearize equations (1)-(5) for nonradial modes of perturbations and derive a local dispersion relation for thermal instability in a stratified medium. As in §3 for radial modes, our approach is Lagrangian and includes the effects of thermal conduction. Similar analyses have been performed by Malagoli et al. (1987) for Eulerian perturbations, and by Balbus (1988) for Lagrangian perturbations, but without conduction. The effects of a radial mass flow and magnetic fields were studied by Balbus & Soker (1989) and Balbus (1991) using Lagrangian perturbations. We apply Δ to equations (2) and (3) and obtain

$$\frac{d^2 \vec{\xi}}{dt^2} = (\nabla \cdot \vec{\xi}) \nabla \Phi + \frac{1}{\rho} \nabla (P \nabla \cdot \vec{\xi}) - \frac{1}{\rho} \nabla \left(P \frac{\Delta T}{T} \right) - \nabla (\vec{\xi} \cdot \nabla \Phi), \quad (\text{A1})$$

$$\begin{aligned} \left(\frac{P}{\gamma - 1} \frac{d}{dt} + \rho T \mathcal{L}_T \right) \frac{\Delta T}{T} + \left(P \frac{d}{dt} - \rho^2 \mathcal{L}_\rho \right) (\nabla \cdot \vec{\xi}) \\ = \frac{1}{4\pi r^2} \frac{\partial}{\partial r} \Delta L_r + \kappa \nabla_t^2 \left(\Delta T - \xi_r \frac{dT}{dr} \right) - (\nabla_t \cdot \vec{\xi}_t) \nabla \cdot \mathbf{F}, \end{aligned} \quad (\text{A2})$$

where $\vec{\xi}_t$ denotes the tangential component of $\vec{\xi}$ and ∇_t is the tangential gradient

$$\nabla_t \equiv \frac{\hat{\theta}}{r} \frac{\partial}{\partial \theta} + \frac{\hat{\phi}}{r \sin \theta} \frac{\partial}{\partial \phi}, \quad (\text{A3})$$

with $\hat{\theta}$ and $\hat{\phi}$ denoting unit vectors in the polar and azimuthal directions, respectively. Equation (18) linking ΔT and ΔL_r is valid for both radial and nonradial perturbations.

Following Balbus (1988), we assume that the perturbations are of the form (see also Cox 1980)

$$\vec{\xi} = [\hat{r} \xi_r(r) + r \xi_t(r) \nabla_t] Y_{lm}(\theta, \phi) e^{\sigma t}, \quad (\text{A4})$$

where $Y_{lm}(\theta, \phi)$ is the spherical harmonic, satisfying an identity

$$\nabla_t^2 Y_{lm} = -\frac{l(l+1)}{r^2} Y_{lm}. \quad (\text{A5})$$

We assume the same angular and temporal dependences in the other perturbed variables ΔT and ΔL_r ; in what follows, we omit $Y_{lm} e^{\sigma t}$ from all the perturbation variables.

The tangential component of equation (A1) is integrated to give

$$\left[\frac{\rho}{P} \sigma^2 + \frac{l(l+1)}{r^2} \right] r \xi_t = \frac{1}{r^2} \frac{dr^2 \xi_r}{dr} - \frac{\Delta T}{T} + \frac{d \ln P}{dr} \xi_r. \quad (\text{A6})$$

From equations (A4) and (A6), we thus write

$$\begin{aligned}\nabla \cdot \vec{\xi} &= \frac{1}{r^2} \frac{dr^2 \xi_r}{dr} - \frac{l(l+1)}{r} \xi_t \\ &= \frac{1}{D} \left[\frac{1}{r^2} \frac{dr^2 \xi_r}{dr} + (D-1) \left(\frac{\Delta T}{T} - \frac{d \ln P}{dr} \xi_r \right) \right],\end{aligned}\quad (\text{A7})$$

where the dimensionless parameter D , defined by

$$D \equiv 1 + \frac{l(l+1)P}{r^2 \rho \sigma^2}, \quad (\text{A8})$$

measures approximately the square of the ratio of the growth time to the sound crossing time across a tangential wavelength.

Substituting equations (A4) and (A7) into the radial component of equation (A1), we obtain

$$\begin{aligned}\frac{d^2}{dr^2} \left(\frac{\xi_r}{r} \right) &+ \left(\frac{4}{r} + \frac{d \ln P/D}{dr} \right) \frac{d}{dr} \left(\frac{\xi_r}{r} \right) \\ &+ \left[\frac{\rho}{P} \left(\frac{1}{r} \frac{d\Phi}{dr} - 4\pi G \rho_{\text{DM}} - D\sigma^2 \right) + (D-1) \frac{d \ln P}{dr} \frac{d \ln T}{dr} - \frac{d \ln r^3 P}{dr} \frac{d \ln D}{dr} \right] \frac{\xi_r}{r} \\ &= \frac{1}{r} \left[\frac{d}{dr} \left(\frac{\Delta T}{T} \right) + \left(D \frac{d \ln P}{dr} - \frac{d \ln D}{dr} \right) \frac{\Delta T}{T} \right].\end{aligned}\quad (\text{A9})$$

Similarly, equation (A2) becomes

$$\begin{aligned}\frac{1}{4\pi r^2} \frac{d}{dr} \Delta L_r &= \left(\frac{P\sigma}{\gamma-1} + \rho T \mathcal{L}_T \right) \frac{\Delta T}{T} + \frac{l(l+1)}{r^2} (\kappa \Delta T + F_r \xi_r) - \frac{\nabla \cdot \mathbf{F}}{r^2} \frac{dr^2 \xi_r}{dr} \\ &+ D^{-1} (P\sigma - \rho^2 \mathcal{L}_\rho - \rho \mathcal{L}) \left[\frac{1}{r^2} \frac{dr^2 \xi_r}{dr} + (D-1) \left(\frac{\Delta T}{T} - \frac{d \ln P}{dr} \xi_r \right) \right]\end{aligned}\quad (\text{A10})$$

Note that when $D = 1$, corresponding to pure radial modes, equations (A9) and (A10) are reduced to equations (19) and (20), respectively. Subject to proper boundary conditions, equations (A9), (A10), and (21) may be integrated to yield solutions for global nonradial modes, but this is beyond the scope of the present paper.

Let us define the local tangential wavenumber $k_t \equiv [l(l+1)]^{1/2}/r$ and the local radial wavenumber $k_r \equiv d \ln \chi / dr$, where χ refers to any perturbed variable. Let us also focus on local modes which vary rapidly in both radial and tangential directions and grow slowly compared to the sound crossing time across their wavelengths, i.e. $k_r r \gg 1$, $k_r (d \ln P / dr) \gg 1$, and $k_r^2 \sim k_t^2 \gg \rho \sigma^2 / P$ (or $D \gg 1$). Using equation (21) in the following alternative form,

$$\frac{\Delta L_r}{4\pi r^2} = \frac{d}{dr} (\kappa \Delta T + F_r \xi_r) - \xi_r (\nabla \cdot \mathbf{F}), \quad (\text{A11})$$

we simplify equations (A9) and (A10) to

$$- \left(k^2 - D \frac{d \ln P}{dr} \frac{d \ln T}{dr} \right) \xi_r = \left(D \frac{d \ln P}{dr} \right) \frac{\Delta T}{T}, \quad (\text{A12})$$

$$- \left[k^2 F_r + \frac{d}{dr} \nabla \cdot \mathbf{F} - (P\sigma - \rho^2 \mathcal{L}_\rho - \rho \mathcal{L}) \frac{d \ln P}{dr} \right] \xi_r = \left[\frac{\gamma P}{\gamma - 1} (\sigma - \sigma_\infty) + \kappa T k^2 \right] \frac{\Delta T}{T}, \quad (\text{A13})$$

where $k^2 \equiv k_r^2 + k_t^2$ is the amplitude of the total wavenumber and σ_∞ is defined by equation (25). Combining equations (A12) and (A13), we finally obtain equation (30) as a local dispersion relation for nonradial thermal perturbations.

REFERENCES

- Afshordi, N., & Cen, R. 2002 ApJ, 564, 669
- Allen, S. W., Ettore, S., & Fabian, A. C. 2001, MNRAS, 324, 877
- Balbus, S. A. 1986, ApJ, 303, L79
- Balbus, S. A. 1988, ApJ, 328, 395
- Balbus, S. A. 1991, ApJ, 372, 25
- Balbus, S. A., & Soker, N. 1989, ApJ, 341, 611
- Bertschinger, E., & Meiksin, A. 1986, ApJ, 306, L1
- Binney, J., & Cowie, L. L. 1981, ApJ, 247, 464
- Böhringer, H., Belsole, E., Kennea, J., Matsushita, K., Molendi, S., Worrall, D. M., Mushotzky, R. F., Ehle, M., Guainazzi, M., Sakelliou, I., Stewart, G., Vestrand, W. T., Dos Santos, S. 2001, A&A, 365, L181
- Bregman, J. N., & David, L. P. 1988, ApJ, 326, 639
- Brighenti, F., & Mathews, W. G. 2002, ApJ, 573, 542
- Brighenti, F., & Mathews, W. G. 2003, ApJ, 587, 580
- Brüggen, M., & Kaiser, C. R. 2002, Nature, 418, 301
- Carilli, C. L., Taylor, G. B. 2002, ARA&A, 40, 319
- Chandran, B. D. G., & Cowley, S. C. 1998, Phys. Rev. Lett., 80, 3077

- Chandran, B. D. G., Cowley, S. C., Ivanushkina, M., & Sydora, R. 1999, *ApJ*, 525, 638
- Cho, J., Lazarian, A., Honein, A., Knaepen, B., Kassinos, S., & Moin, S. 2003, *ApJ*, 589, L77
- Chun, E., & Rosner, R. 1993, *ApJ*, 408, 678
- Churazov, E., Sunyaev, R., Forman, W., & Böhringer, H. 2002, *MNRAS*, 332, 729
- Ciotto, L., & Ostriker, J. P. 2001, *ApJ*, 551, 131
- Cox, J. P. 1980, *Theory of Stellar Pulsations* (Princeton: Princeton Univ. Press)
- David, L. P., Hughes, J. P., & Tucker, W. H. 1992, *ApJ*, 394, 452
- David, L. P., Nulsen, P. E. J., McNamara, B. R., Forman, W., Jones, C., Ponman, T., Robertson, B., & Wise, M. 2001, *ApJ*, 557, 546
- Defouw, R. J. 1970, *ApJ*, 160, 659
- Dupke, R., & White, R. E., III. 2003, *ApJ*, 583, L13
- Ettori, S., Fabian, A. C., Allen, S. W., & Johnstone, R. M. 2002, *MNRAS*, 331, 635
- Fabian, A. C. 1994, *ARA&A*, 32, 277
- Fabian, A. C., Mushotzky, R. F., Nulsen, P. E. J., & Peterson, J. R. 2001a, *MNRAS*, 321, L20
- Fabian, A. C., Sanders, J. S., Ettori, S., Taylor, G. B., Allen, S. W., Crawford, C. S., Iwasawa, K., & Johnstone, R. M. 2001b, *MNRAS*, 321, L33
- Fabian, A. C., Voigt, L. M., & Morris R. G. 2002, *MNRAS*, 335, L71
- Field, G. B. 1965, *ApJ*, 142, 531
- Gaetz, T. J. 1989, *ApJ*, 345, 666
- Goldreich, P., & Sridhar, S. 1995, *ApJ*, 438, 763
- Goldreich, P., & Sridhar, S. 1997, *ApJ*, 485, 680
- Gruzinov, A. 2002, *astro-ph/0203031*
- Johnstone, R. M., Allen, S. W., Fabian, A. C., & Sanders, J. S. 2002, *MNRAS*, 336, 299

- Kaiser, C. R., Binney, J. 2003, MNRAS, 338, 837
- Kitayama, T., & Suto, Y. 1996, ApJ, 469, 480
- Loewenstein, M., Zweibel, E. G., & Begelman, M. C. 1991, ApJ, 377, 392
- Malagoli, A., Rosner, R., & Bodo, G. 1987, ApJ, 319, 632
- Malyshkin, L., & Kulsrud, R. 2001, ApJ, 549, 402
- Maoz, D., Rix, H.-W., Gal-Yam, A., & Gould, A. 1997, ApJ, 486, 75
- Markevitch, M. et al. 2000, ApJ, 541, 542
- Markevitch, M. et al. 2003, ApJ, 586, L19
- Matsushita, K., Belsole, E., Finoguenov, A., & Böhringer, H. 2002, A&A, 386, 77
- Mazzotta, P., Vikhlinin, A., Fusco-Femiano, R., & Markevitch, M. 2002, ApJ, 569, L31
- McKee, C. F., & Begelman, M. C. 1990, ApJ, 358, 392
- Molendi, S., & Pizzolato, F. 2001, ApJ, 560, 194
- Nagai, D., & Kravtsov, A. V. 2003, ApJ, 587, 514
- Narayan, R., & Medvedev, M. V. 2001, ApJ, 562, L129
- Peterson, J. R., Paerels, F. B. S., Kaastra, J. S., Arnaud, M., Reiprich, T. H., Fabian, A. C., Mushotzky, R. F., & Jernigan, J. G., Sakelliou, I. 2001, A&A, 365, L104
- Peterson, J. R., Kahn, S. M., Paerels, F. B. S., Kaastra, J. S., Tamura, T., Bleeker, J. A. M., Ferrigo, C., & Jernigan, J. G. 2003, ApJ, 590, 207
- Pistinner, S., & Shaviv, G. 1996, ApJ, 459, 1
- Press, W. H., Teukolsky, S. A., Vetterling, W. T., & Flannery, B. P. 1992, Numerical Recipes in Fortran (Cambridge: Cambridge Univ. Press), 838
- Rechester, A. B., & Rosenbluth, M. N. 1978, Phys. Rev. Lett., 40, 38
- Reynolds, C. S., Heinz, S., & Begelman, M. C. 2002, MNRAS, 332, 271
- Roettiger, K., Stone, J. M., & Mushotzky, R. F. 1998, ApJ, 493, 62
- Rosati, P., Borgani, S., & Norman, C. 2002, ARA&A, 40, 539

- Rosner, R., & Tucker, W. H. 1989, *ApJ*, 338, 761
- Ruszkowski, M., & Begelman, M. C. 2002, *ApJ*, 581, 223
- Rybicki, G. B., & Lightman, A. P. 1979, *Radiative processes in astrophysics* (New York: Wiley)
- Sarazin, C. L. 1988, *X-ray emissions from clusters of galaxies* (Cambridge: Cambridge University Press)
- Shapiro, S. L., & Teukolsky, S. A. 1983, *Black Holes, White Dwarfs, and Neutron Stars* (New York: Wiley-Interscience), pp 127-147
- Soker, N. 2003, *MNRAS*, 342, 463
- Spitzer, L. 1962, *Physics of Fully Ionized Gases* (New York: Interscience)
- Stone, J. M., & Norman, M. L. 1992, *ApJS*, 80, 753
- Tamura, T., Kaastra, J. S., Peterson, J. R., Paerels, F. B. S., Mittaz, J. P. D., Trudolyubov, S. P., Stewart, G., Fabian, A. C., Mushotzky, R. F., Lumb, D. H., & Ikebe, Y. 2001, *A&A*, 365, L87
- Tucker, W. H., & Rosner, R. 1983, *ApJ*, 267, 547
- White, R. E., III, & Sarazin, C. L. 1987, *ApJ*, 318, 612
- Vikhlinin, A., Markevitch, M., & Murray, S. S. 2001a, *ApJ*, 549, L47
- Vikhlinin, A., Markevitch, M., & Murray, S. S. 2001b, *ApJ*, 551, 160
- Voigt, L. M., Schmidt, R. W., Fabian, A. C., Allen, S. W., Johnstone, R. M. 2002, *MNRAS*, 335, L7
- Zakamska, N. L., & Narayan, R. 2003, *ApJ*, 582, 162 (ZN03)

Table 1. Parameters and Time Scales for Five Clusters.

Name	$T(0)$ (keV) ^a	$n_e(0)$ (cm ⁻³) ^a	f^a	t_{cool} (Gyr) ^b	t_{grow} (Gyr) ^c	$t_{\text{grow}}/t_{\infty,0}$ ^{c,d}
Abell 1795	2	0.049	0.2	0.98	4.1	6.3
Abell 1835	5	0.17	0.4	0.45	1.9	6.3
Abell 2199	1.6	0.074	0.4	0.58	3.5	9.0
Abell 2390	4	0.069	0.3	0.98	4.6	7.1
RXJ 1347.5-1145	6	0.11	0.3	0.76	3.3	6.2

^aAdopted from ZN03.

^b t_{cool} is the isobaric cooling time at the cluster center (see eq. [8]).

^c t_{grow} is the growth time of the global radial mode.

^d $t_{\infty,0}$ is the growth time of the local isobaric thermal instability at the cluster center in the absence of conduction (see eq. [27]).

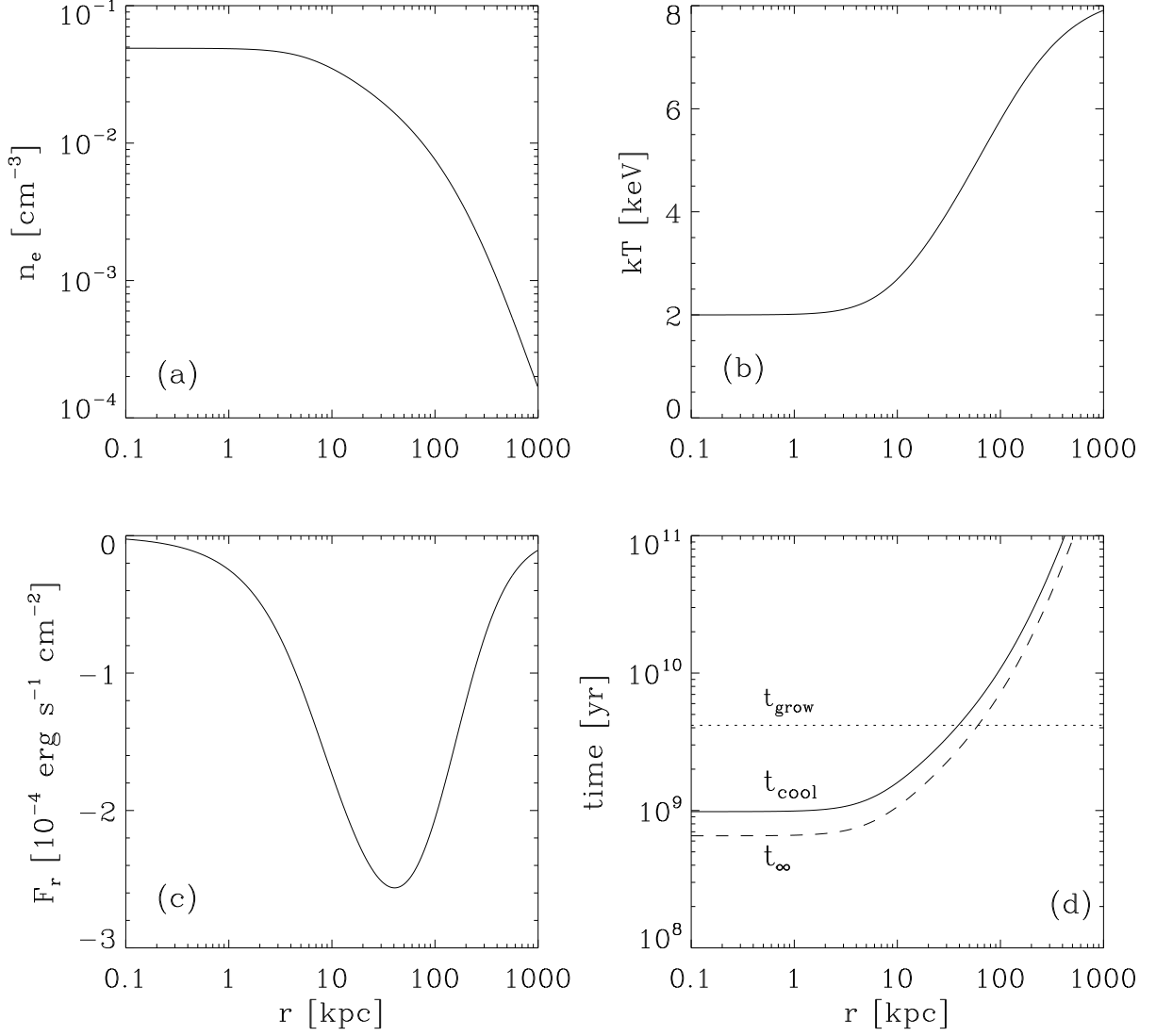


Fig. 1.— (a) Density, (b) temperature, (c) radial heat flux, and (d) isobaric cooling time (t_{cool} , solid line, see eq. [8]) of a model of A1795 with conduction. The chosen parameters are $f = 0.2$, $T(0) = 2$ keV, $n_e(0) = 0.049$ cm⁻³, $M_0 = 6.6 \times 10^{14} M_{\odot}$, and $r_s = 20r_c = 460$ kpc (ZN03). Shown also in (d) are the growth times of local (t_{∞} , dashed, see eq. [27]) and global (dotted) thermal instability.

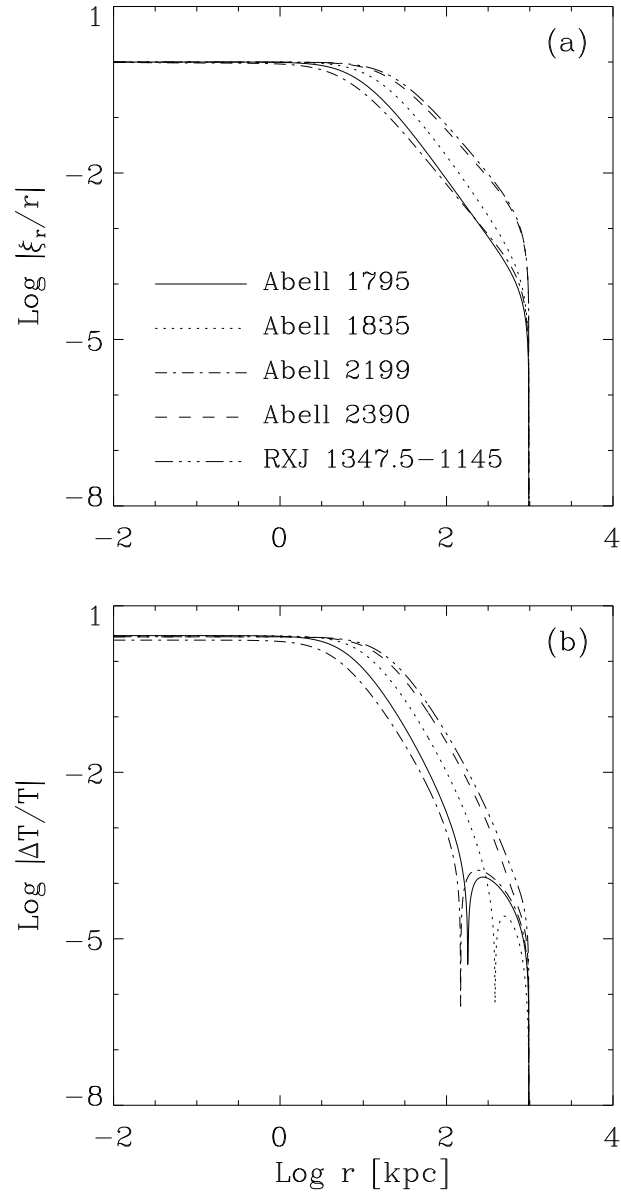


Fig. 2.— Eigenfunctions of the radial unstable mode for five clusters, plotted as functions of radius. Note that the amplitudes of the solutions are largest near the center and decrease very rapidly as r increases.

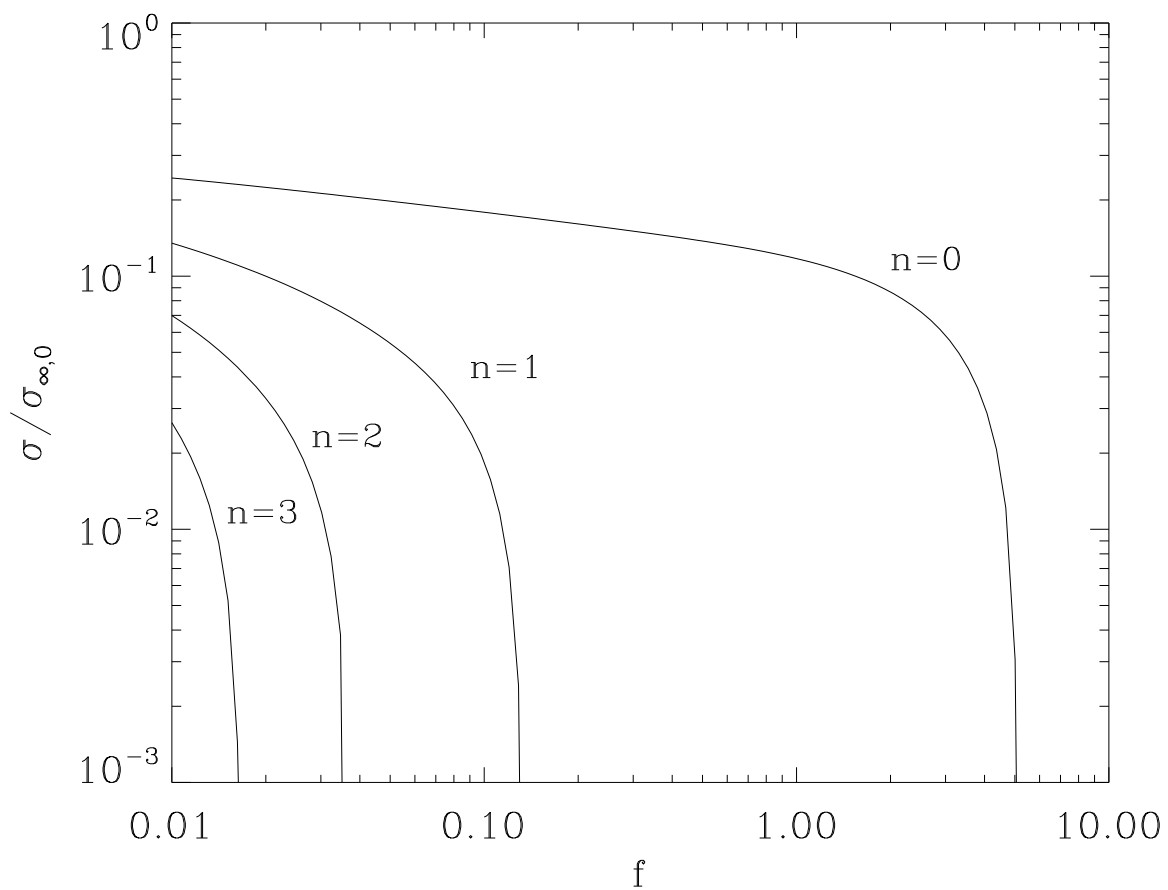


Fig. 3.— Effect of thermal conductivity on the growth rates of global unstable modes in A1795. The abscissa is the reduction factor f of thermal conductivity applied to perturbations, while the ordinate is the eigenfrequency normalized by $\sigma_{\infty,0} = (0.64 \text{ Gyr})^{-1}$, the growth rate of the local isobaric instability at the cluster center. Each curve is labeled by n , the number of nodes in the corresponding eigenfunction $\xi_{r,n}/r$. See text for details.

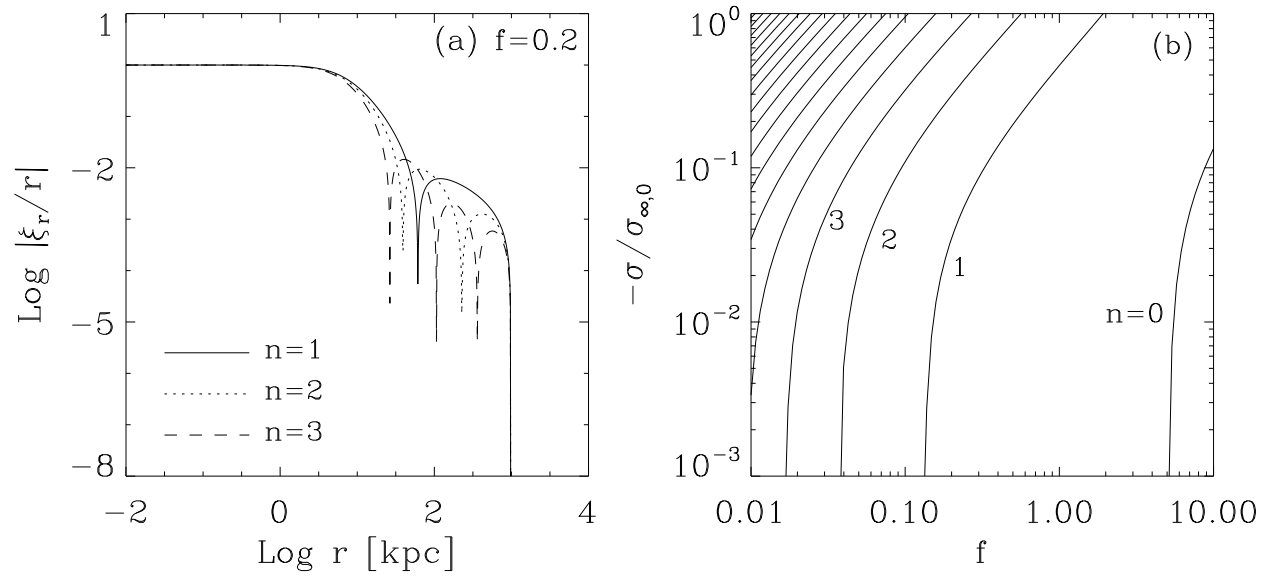


Fig. 4.— (a) Examples of eigenfunctions for decaying modes ($\sigma < 0$) in A1795 with $f = 0.2$ (b) The effect of thermal conductivity on the decay rates of modes. Higher-order modes have larger decay rates.

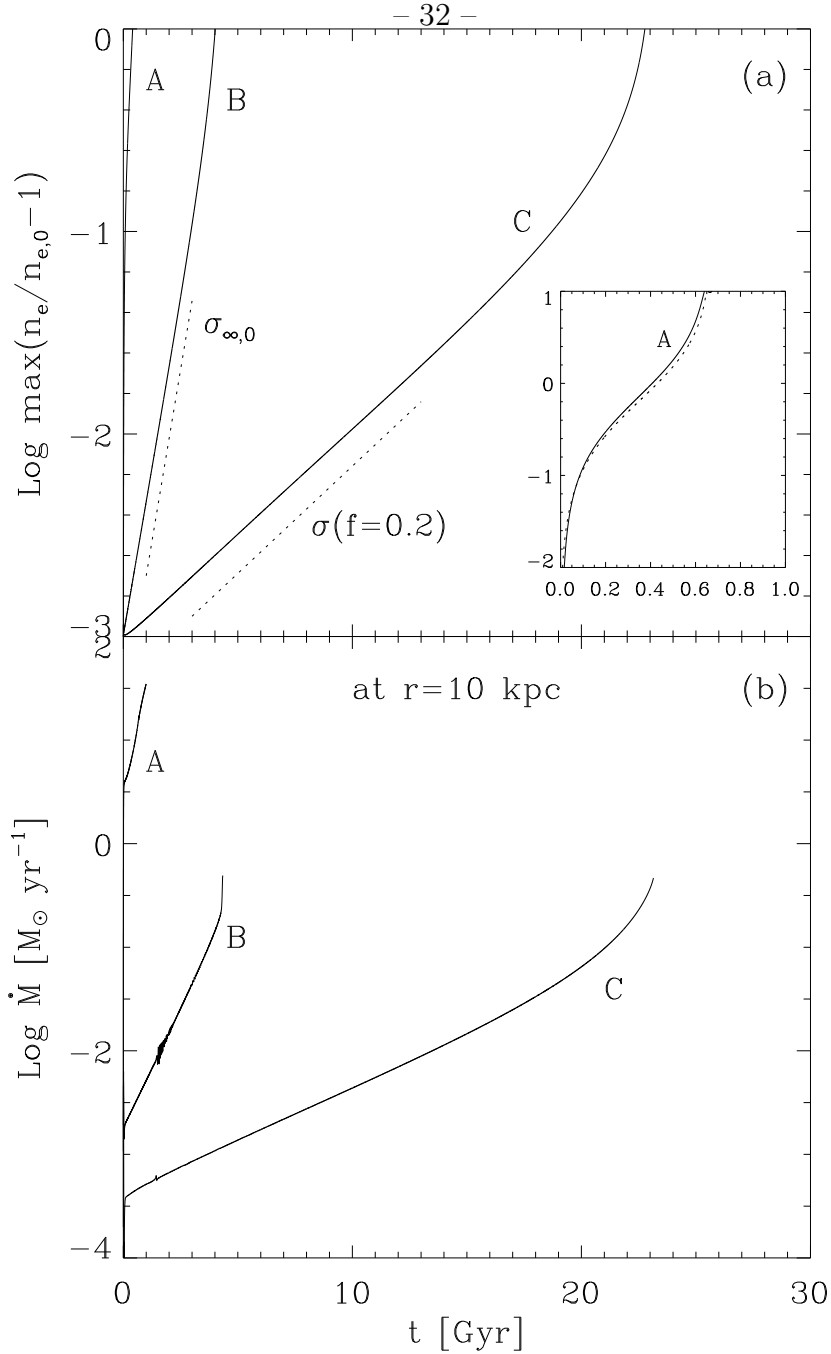


Fig. 5.— Time evolution of (a) maximum density and (b) mass inflow rate measured at $r = 10$ kpc in models A-C. The two dotted lines in (a) represent the maximum growth rates, $\sigma(f = 0.2) = (4.1 \text{ Gyr})^{-1}$ and $\sigma_{\infty,0} = (0.64 \text{ Gyr})^{-1}$, of thermal instability with and without conduction as estimated from the linear analysis. As expected, these lines agree well with the time evolutions of Models B and C. The insert in (a) compares the evolution of the maximum density in model A (solid line) with the analytic prediction, $n_e(t)/n_e(0) = (1 - 3t/2t_{\text{cool}})^{-2/3}$, for isobaric cooling (dotted line). See text for details.

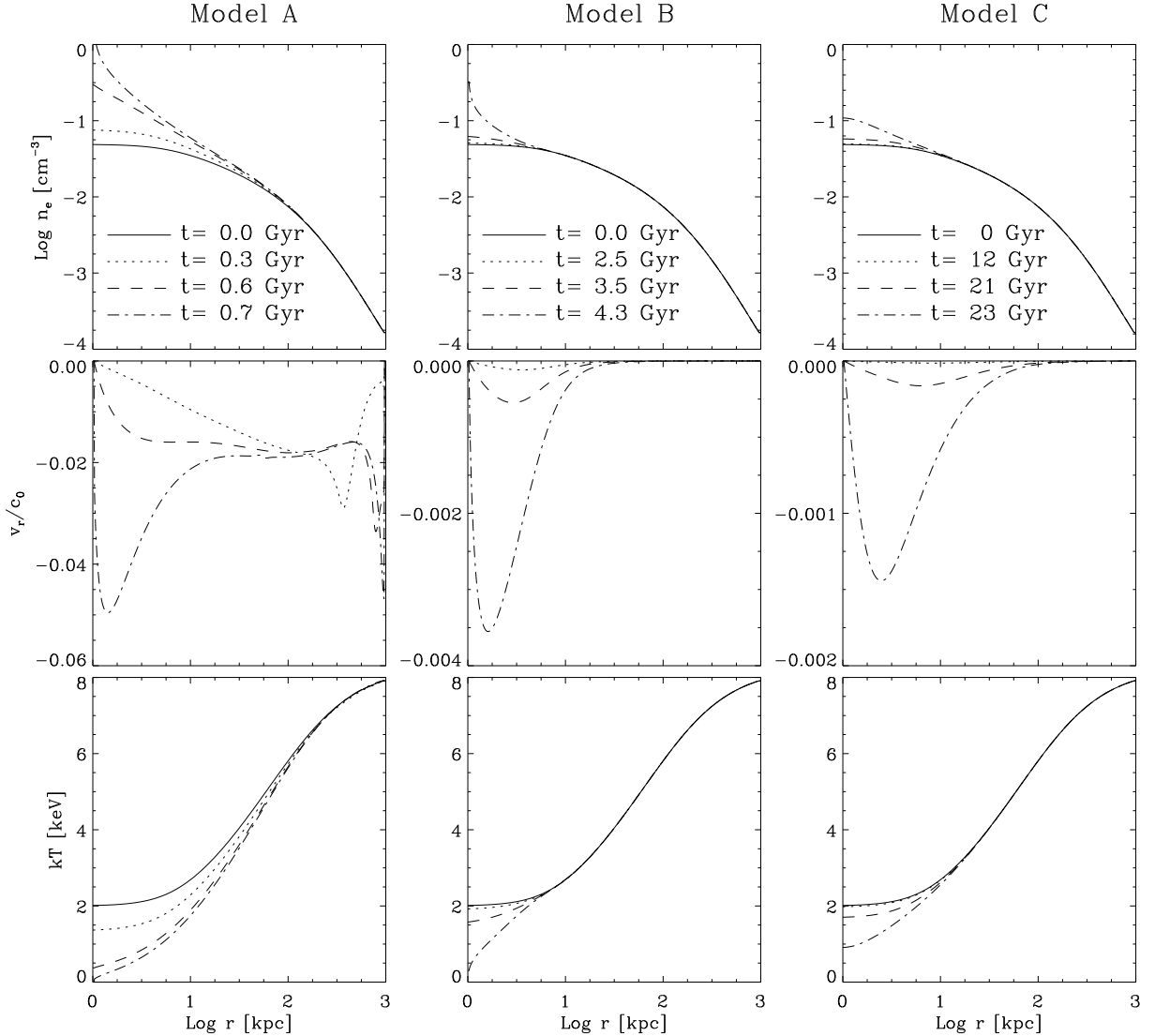


Fig. 6.— Evolution of (*top row*) electron number density, (*middle row*) radial velocity in units of the central sound speed $c_0 = 390 \text{ km s}^{-1}$, and (*bottom row*) temperature, for models A-C. *Left:* Strong radiative cooling in model A quickly leads to an inward cooling flow, which causes the central density to increase by more than three orders of magnitude in 0.9 Gyr. *Middle:* Model B, which is initially in equilibrium but has no conduction, has perturbations that grow at a rate σ_∞ , driving the system into a highly nonlinear state in less than 5 Gyr. *Right:* Thermal conduction in model C delays the development of thermal instability significantly. Even after 20 Gyr, the density and temperature profiles are not very different from the initial ones.